Original Research

The Impact of Operating Conditions on the Performance of a CH$_4$ Dry Reforming Membrane Reactor for H$_2$ Production

Akira Nishimura [1, *], Satoshi Ohata [2], Kaito Okukura [3], Eric Hu [4]

1. Division of Mechanical Engineering, Graduate School of Engineering, Mie University, 1577 Kurimamachiya-cho, Tsu, Mie, 514-8507 Japan; E-Mail: nisimura@mach.mie-u.ac.jp
2. Division of Mechanical Engineering, Graduate School of Engineering, Mie University, 1577 Kurimamachiya-cho, Tsu, Mie, 514-8507 Japan; E-Mail: 420M111@m.mie-u.ac.jp
3. Division of Mechanical Engineering, Graduate School of Engineering, Mie University, 1577 Kurimamachiya-cho, Tsu, Mie, 514-8507 Japan; E-Mail: 419M109@m.mie-u.ac.jp
4. School of Engineering, the University of Adelaide, Adelaide, SA 5005, Australia; E-Mail: eric.hu@adelaide.edu.au

* **Correspondence:** Akira Nishimura; E-Mail: nisimura@mach.mie-u.ac.jp

Academic Editor: Alfonso Chinnici

Special Issue: Hydrogen Energy: Sustainable Production, Storage and Utilisation

Abstract

Biogas is a promising resource for the production of H$_2$ since it liberates energy by recycling waste, along with the reduction of CO$_2$. In this paper, the biogas dry reforming membrane reactor is proposed to produce H$_2$ for use in fuel cells. Pd/Cu alloy membrane is used to enhance the performance of the biogas dry reforming reactor. This study aims at understanding the effect of operating parameters such as feed ratio of sweep gas, pressure in the reactor, and reaction temperature on the performance of the biogas dry reforming membrane reactor. The effect of the molar ratio of the supplied CH$_4$:CO$_2$, feed ratio of the sweep gas, and the valve located at the outlet of the reaction chamber on the performance of biogas dry reforming are investigated. Besides, the thermal efficiency of the proposed reactor is also evaluated. The results show that the concentration of H$_2$ in the closed valve

condition is higher than that of the open valve, and the optimum feed ratio of the sweep gas to produce H_2 is 1, irrespective of the molar ratio of supplied CH_4:CO_2. Also, H_2 selectivity and CO selectivity increases and decreases respectively when the reaction temperature increases, irrespective of the molar ratio of supplied CH_4:CO_2. Therefore, the thermal efficiency of the closed valve is higher than that of the opened valve. Also, the thermal efficiency is the maximum when the feed ratio of the sweep gas is 1 due to high H_2 production performance.

1. Introduction

The fuel cell is a promising power generation technology as environmentally toxic gases such as NO_x, SO_x, and CO_2 are not emitted. H_2 is fuel for the fuel cell, produced from different resources. However, CO_2 would be emitted upon the production of H_2 from fossil fuels such as coal, oil, and natural gas. Therefore, H_2 production technology without CO_2 emission is important in a sustainable world.

In this study, H_2 is produced from biogas. Biogas is a gaseous fuel consisting of CH_4 (55–75 vol%) and CO_2 (25–45 vol%) [1], mainly produced upon fermentation of CH_4 by the action of anaerobic microorganisms on raw materials such as garbage, livestock excretion, and sewage sludge. Besides, the conversion of biogas to H_2 is carbon neutral, thus reduces carbon footprint. From a recent report by the World Bioenergy Association based on the data from the International Energy Agency (IEA) [2], the domestic supply of biogas globally reached 1.33 EJ in 2017 from 0.28 EJ in 2000. Therefore, biogas is a promising energy resource for the future.

Biogas is usually used as a fuel in the gas engine or micro gas turbine [3]. Since biogas contains CO_2 of approximately 40 vol%, the heating value is low compared to natural gas, which results in a decrease in the efficiency of power generation. Therefore, in this study, biogas is used in the dry reforming process to produce H_2, which is used as fuel for the fuel cells. Biogas dry reforming to produce H_2 was previously studied by several researchers [4–17]. The catalyst used in the process is important in evaluating the performance of biogas dry reforming. Though some unique catalysts such as Fe/Al_2O_3 [4], Rh/Al_2O_3 [5], $Co-Ce/ZrO_2$ [6], and Fe_2O_3/zeolite [7] are used, Ni-based catalyst is the most common one for the biogas dry reforming process [8–17], which is also used in this study. This study adopts a membrane reactor to improve the efficiency of biogas dry reforming. Generally, a membrane reactor is used to improve the CH_4 steam reforming by separating H_2 from the reaction space [18–20] as soon as it is produced. The synergetic effect of the membrane reactor on performing the reaction and separation in the same unit, their simplicity, and the possibility of advanced levels of automation and control offer an attractive opportunity to redesign industrial processes [21]. Generally, Pd based membrane is used to separate H_2 due to its high efficiency [21–23]. Some studies used the membrane reactor for CH_4 dry reforming [21–29]. The coupled effect of the membrane and catalyst on CH_4 conversion was discussed earlier [21]. It

was reported that the dense Pd/Ag/Cu alloy membrane and $Ni/CeZrO_2$ catalyst together had the highest CH_4 conversion of 65.2% [22] among the investigated combinations. The Pd/Au alloy membrane used in the two-zone fluidized bed reactor [23, 29] showed the CH_4 conversion and H_2 selectivity to be higher compared to the conventional fluidized bed reactor. The highest CH_4 conversion and H_2/CO ratio were approximately 80% and 1.8, respectively. Ni was not only used in the membrane reactor but also as a catalyst to promote the CH_4 dry reforming process in the same reactor [24]. Though the CH_4 conversion and H_2 recovery achieved up to 85% and 70%, respectively, the equilibrium conversion was not achieved due to the limited resistance time in the reactor. The numerical simulation using the double tube reactor model investigated the percentage of CH_4 conversion, H_2 concentration, and temperature in the CH_4 dry reforming membrane reactor [27]. It was found that high reformer temperature in the membrane reactor was not favorable for the high production of H_2. Besides, the impact of the number of layers of the membrane on H_2 separation, as well as CH_4 and CO_2 conversion in the dry reforming process was investigated by numerical simulation [30]. The CH_4 and CO_2 conversion decreased as the number of layers increased, although the inclination slightly changed after six layers of the membrane. The permeation of H_2 into the membrane increased as the number of layers increased. The gas separation membrane was also applied to the steam reforming of CH_4 [31] and C_2H_5OH [32]. CO_2 capture by dual-phase ceramic-carbonate was effective in obtaining highly pure H_2, and achieved higher CO_2 recovery compared to the conventional fixed bed reactor. The Pd/Cu membrane reactor with Ir/CeO_2 catalyst provided a high H_2 yield of 98.1% at 550 °C and a reforming pressure of 1300 kPa [32]. This membrane was used with Ru or Rh catalyst [33], and evaluated at 550 °C, resulting in the CH_4 and CO_2 conversion of 8% to 40%. These values were slightly higher than those obtained for a fixed bed reactor with the same amount of catalyst.

However, the impact of gas separation conditions such as feed ratio of the sweep gas, reactor pressure, and varying reaction temperature on the performance of biogas dry reforming reactor is currently unknown.

Therefore, this study aims to understand the effect of operating conditions such as feed ratio of the sweep gas, pressure in the reactor, and reaction temperature on the performance of biogas dry reforming. Since a pure Pd membrane has a relatively high solubility for carbon, it causes membrane degradation leading to the loss of permeability [34]. Therefore, the Pd/Cu alloy membrane was used in this study. The reaction scheme of CH_4 dry reforming is as follow:

$$CH_4 + CO_2 \rightarrow 2CO + 2H_2 \qquad \Delta H_{298}^o = 247 \text{ kJ/mol} \qquad (1)$$
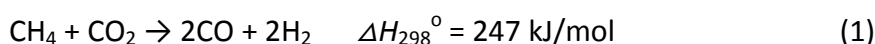
2. Experiment

2.1 Experiment Set-Up

Figure 1 illustrates the experimental set-up used in this study. It consists of a gas cylinder, mass flow controller (S48-32; produced by HORIBA METRON INC.), pressure sensor (KM31; by NAGANO KEIKI), valve, reactor, i.e., a combination of the reaction chamber and sweep chamber, and gas sampling tap. The reactor is in the furnace where the temperature is controlled by the far-infrared heater (MCHNNS1; produced by MISUMI). CH_4 gas with purity over 99.4 vol% and CO_2 gas with purity over 99.9 vol% are controlled by mass flow controller and mixed before passing through the reactor. The pressure of the mixed gas is measured by the pressure sensor. Ar gas having a purity

over 99.99 vol% is controlled by the mass flow controller, and measured by the pressure sensor. This is fed as a sweep gas. The exhausted gas at the outlet of the reactor is suctioned by a gas syringe via the gas sampling tap, and its concentration is measured by FID gas chromatography and a methanizer. The minimum resolution of both the FID gas chromatograph and methanizer is 1 ppmV. The gas pressure at the outlet of the reactor is measured using the pressure sensor. The gas concentration and pressure are measured at the outlet of the reaction chamber and sweep chamber, respectively. A valve is installed next to the pressure gauge at the outlet of the reaction chamber to investigate the effect of pressure on the performance of the dry reforming of CH_4. The valve is placed 65 cm away from the outlet of the reaction chamber. Though its position would better be near the outlet, this distance is kept due to the heat resistance of the pressure sensor installed before the valve. When the valve is closed, the gas in the reaction chamber flows to the sweep chamber preferentially.
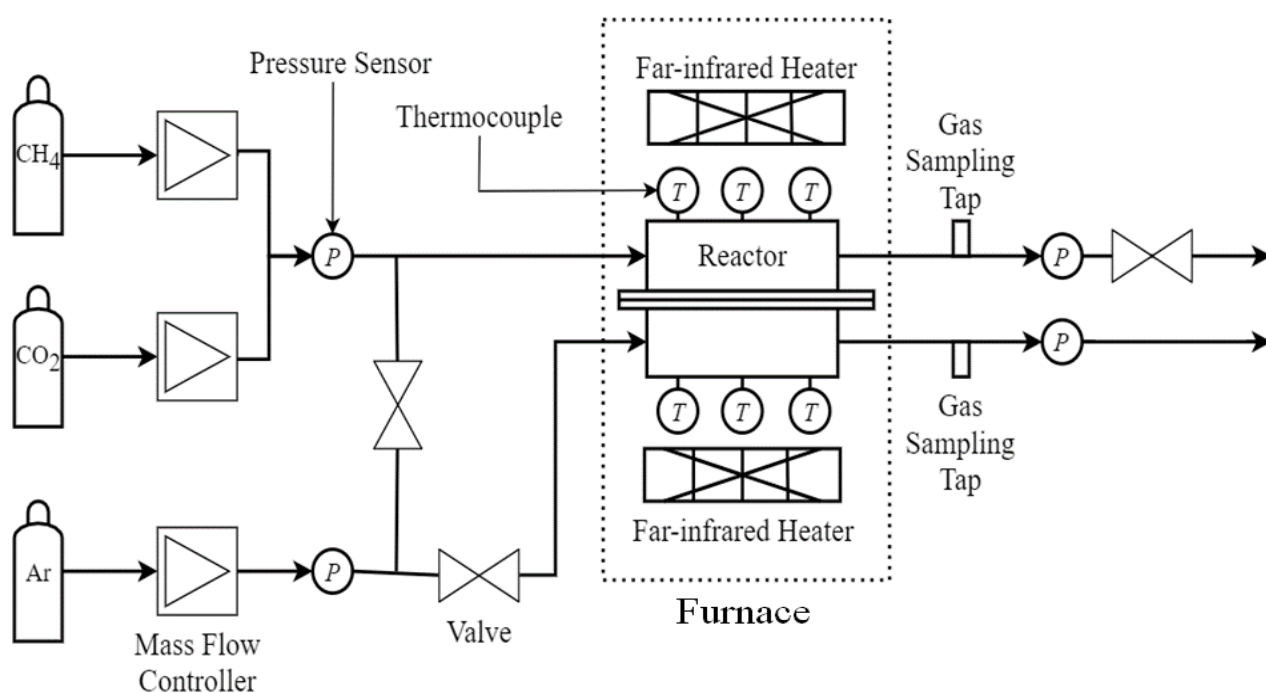

Figure 1 Schematic drawing of the experimental set-up.

Figure 2 illustrates the details of the reactor. The reactor consists of the reaction chamber, sweep chamber, and H_2 separation membrane. The reaction chamber and sweep chamber are made of stainless steel, having dimensions 40 mm × 100 mm × 40 mm. The volume of the reaction space is $16 × 10^{-5}$ m^3. Pure Ni catalyst having a porous structure is placed in the reaction chamber, which means the catalyst is 100 wt% of Ni. The average pore diameter of this catalyst is 1.9 mm. The weight of the Ni catalyst is 63.1 g. The Pd/Cu alloy membrane (Cu of 40 wt%; produced by Tanaka Kikinzoku Kogyo), which is installed between the reaction and separation chambers, causes H_2 separation. The thickness of the Pd/Cu alloy membrane is 20 mm. The temperatures at the inlet, middle, and outlet of the reaction and sweep chambers are measured by K-type thermocouples. The measured temperature and pressure are collected by the data logger (GL240; by Graphtec Corporation).
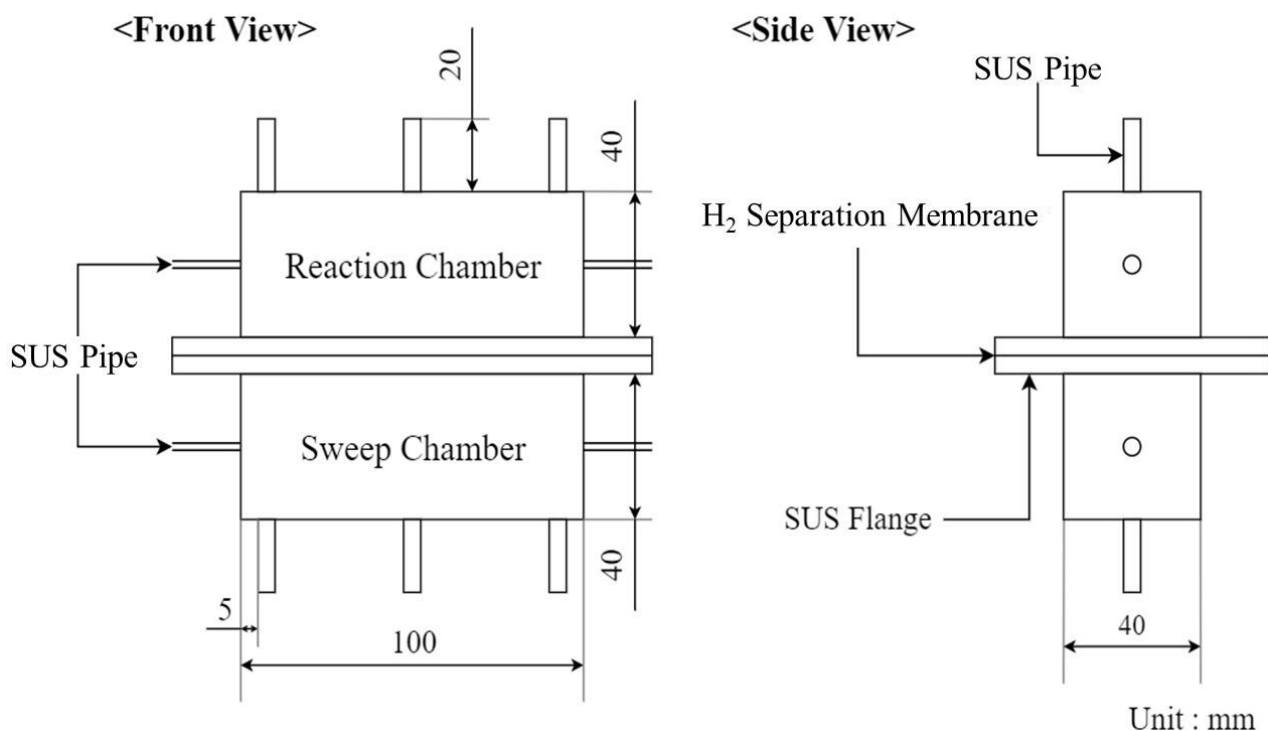
Figure 2 Schematic drawing of reactor.

Table 1 lists the experimental conditions. The molar ratio of the supplied $CH_4:CO_2$ varies at 1.5:1, 1:1, or 1:1.5 since this ratio simulates the biogas. The feed ratio of the sweep gas, which is defined as the flow rate of sweep gas divided by the flow rate of supply gas composed of CH_4 and CO_2, is set to 0.5, 1, or 2. The effects of these ratios, in the conditions when the valve is open or close and the reaction temperatures of 400 °C, 500 °C and 600 °C, were studied. The gas concentrations in the reaction and sweep chambers were evaluated by FID gas chromatograph, and methanizer (produced by GL Science). This study shows the average data of ten trials for different experimental conditions in the following figures. The distribution of each of the gas concentration was below 10%. H_2 and CO selectivity were evaluated. The thermal efficiency of the proposed reactor was also evaluated.

Table 1 Experimental condition.

Reaction temperature [°C]	400, 500, 600
Pressure of supply gas [MPa]	0.3
Temperature of supply gas [°C]	25
Molar ratio of supplied $CH_4 : CO_2$ (Flow rate of CH_4 and CO_2 [NL/min])	1.5 : 1, 1 : 1, 1 : 1.5 (1.088 : 0.725, 0.725 : 0.725, 0.725 : 1.088)
Feed ratio of sweep gas	0.5, 1, 2
State of valve installed at the outlet of reaction chamber	open, closed

2.2 Evaluation Procedure of Performance of the Proposed Reactor

In this study, the performance of the proposed reactor is evaluated in terms of gas concentration at the outlet of the reaction and sweep chambers, pressure difference between the gas and sweep chambers, H_2 and CO selectivity, and thermal efficiency. H_2 and CO selectivities are defined as follows:

$$S_{H2} = C_{H2, out}/(C_{H2, out} + C_{CO, out}) \times 100 \qquad (2)$$
$$S_{CO} = C_{CO, out}/(C_{H2, out} + C_{CO, out}) \times 100 \qquad (3)$$

where S_{H2} is the H_2 selectivity (%), $C_{H2, out}$ is the concentration of H_2 at the outlet of the reaction and sweep chambers (ppmV), $C_{CO, out}$ is the concentration of CO at the outlet of the reaction chamber (ppmV), and S_{CO} is the CO selectivity (%). The thermal efficiency is defined as follows:

$$\eta = Q_{H2}/(Q_{react} + Q_{sweep}) \times 100 \qquad (4)$$
$$Q_{H2} = \{(m_{CH4} + m_{CO2})/(22.4 \times 60)\} \times (C_{H2, out}/10^6) \times (H_l \times 22.4 \times 10^3) \qquad (5)$$
$$Q_{react} = Q_{CH4} + Q_{CO2} \qquad (6)$$
$$Q_{CH4} = \{(m_{CH4}/(22.4 \times 60)\} \times C_{p, CH4} \times (T_{react} - T_{room}) \qquad (7)$$
$$Q_{CO2} = \{(m_{CO2}/(22.4 \times 60)\} \times C_{p, CO2} \times (T_{react} - T_{room}) \qquad (8)$$
$$Q_{sweep} = \{(m_{Ar}/(22.4 \times 60)\} \times C_{p, Ar} \times (T_{react} - T_{room}) \qquad (9)$$

where η is the thermal efficiency (%), Q_{H2} is the heating value of produced H_2 (W), m_{CH4} is the flow rate of CH_4 at the inlet of the reaction chamber (NL/min), m_{CO2} is the flow rate of CO_2 at the inlet of the reaction chamber (NL/min), H_l is the low heating value of H_2 (= 10.79) (MJ/Nm^3), Q_{react} is the heat required for the reaction gases (W), Q_{CH4} is the heat needed to preheat the supplied CH_4 (W), Q_{CO2} is the heat needed to preheat the supplied CO_2 (W), $C_{p, CH4}$ is the specific heat of CH_4 (kJ/(kmol · K)), T_{react} is the reaction temperature (K), T_{room} is the room temperature (K), $C_{p, CO2}$ is the specific heat of CO_2 (kJ/(kmol · K)), Q_{sweep} is the heat needed to preheat sweep gas (W), m_{Ar} is the flow rate of Ar at the inlet of the sweep chamber (NL/min), and $C_{p, Ar}$ is the specific heat of CO_2 (kJ/(kmol · K)).
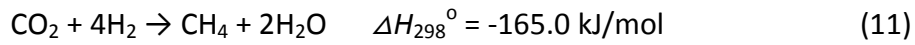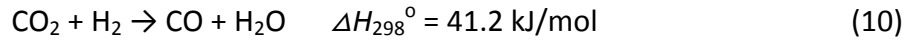
3. Results and Discussion

3.1 Effect of Feed Ratio of Sweep Gas and Pressure in Reaction Chamber on H_2 Production

Figure 3, Figure 4, Figure 5 and Figure 6 compare the relationship between the concentration of CH_4, CO_2, H_2, and CO at the outlet of the reaction chamber, and the feed ratio of sweep gas, when the valve installed at the outlet is open or close, respectively. Figure 7 shows the comparison of the relationship between the concentration of H_2 at the outlet of the sweep chamber and feed ratio of sweep gas when the valve installed at the outlet of the reaction chamber is open or close, respectively. In these figures, the feed ratio of sweep gas is indicated by $m_{Ar}/(m_{CH4}+m_{CO2})$. The molar ratio of the supplied CH_4:CO_2 is 1.5:1. The reaction temperature is varied to 400 °C, 500 °C, or 600 °C.

According to Figure 4 and Figure 5, the concentration of CO_2 and H_2 in the reaction chamber are lower and higher, respectively, when the valve is close. Since the pressure difference between the reaction and sweep chambers is higher upon closing the valve, it is thought that H_2 separation is

promoted, increasing the concentration of H_2. The increase in the H_2 concentration in the sweep chamber is shown in Figure 7. Though the concentration of CO_2 decreased, those of CH_4 (Figure 3) and CO (Figure 6) increased, when the valve is close. The following reactions [8, 12] would take place:

$$CO_2 + H_2 \rightarrow CO + H_2O \qquad \Delta H_{298}^{o} = 41.2 \text{ kJ/mol} \qquad (10)$$
$$CO_2 + 4H_2 \rightarrow CH_4 + 2H_2O \qquad \Delta H_{298}^{o} = -165.0 \text{ kJ/mol} \qquad (11)$$

According to the reactions shown in Eq (10) and (11), CH_4 and CO consumption increased upon consumption of CO_2 and H_2.
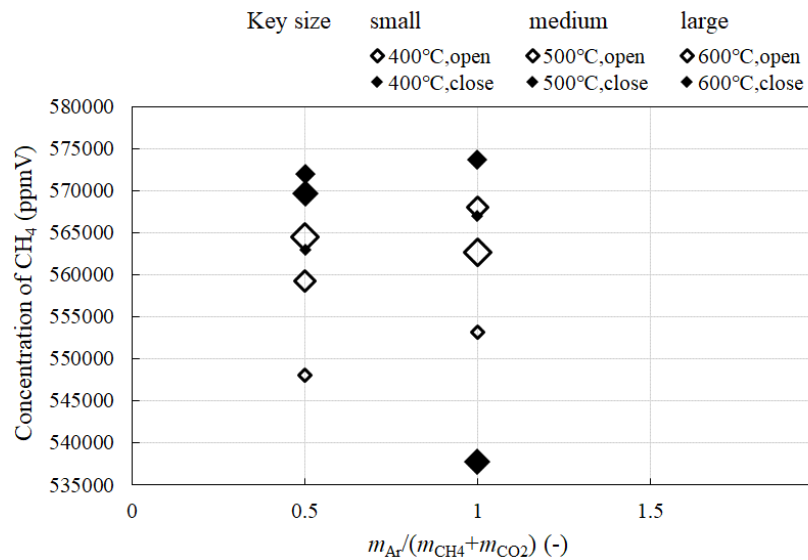

Figure 3 Comparison of the relationship between the concentration of CH_4 at the outlet of the reaction chamber and feed ratio of sweep gas with the valve open or close ($CH_4 : CO_2 = 1.5 : 1$).
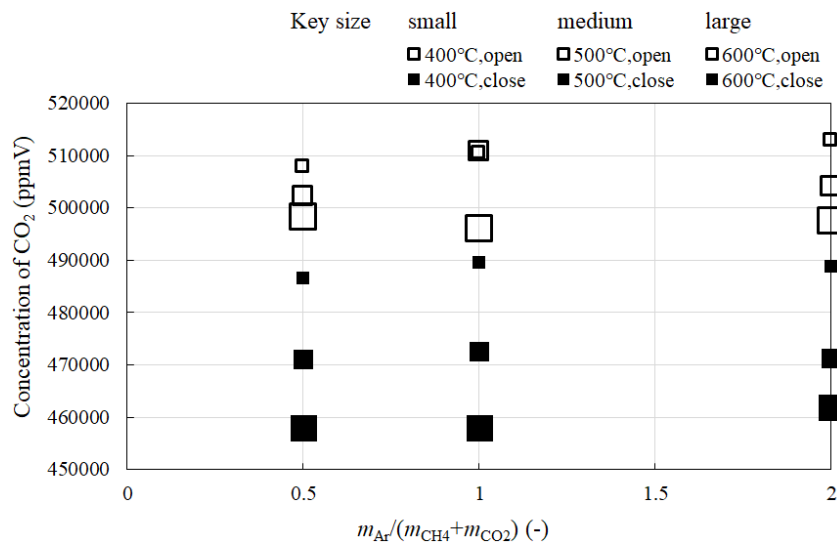

Figure 4 Comparison of the relationship between the concentration of CO_2 at the outlet of the reaction chamber and feed ratio of sweep gas with the valve open or close ($CH_4 : CO_2 = 1.5 : 1$).

Besides, the highest concentration of H_2 is obtained for $m_{Ar}/(m_{CH4}+m_{CO2}) = 1$, according to Figure 5, Figure 6 and Figure 7. It is revealed that the optimum $m_{Ar}/(m_{CH4}+m_{CO2})$ to produce H_2 is 1. This result agrees with a previous study [22]. According to this [22], since the main CH_4 dry reforming reaction, i.e., Eq (1) is reversible, introducing excess amounts of reactants could drive the reaction forward, resulting in the generation of more H_2. However, the produced H_2 could also react with the unreacted CO_2 in the reversible water-gas shift reactions, i.e., Eqs. (10) and (11). Therefore, higher CO_2 consumption was observed compared to that of CH_4. As a result, the highest concentration of H_2 was obtained when $m_{Ar}/(m_{CH4}+m_{CO2}) = 1$, as the reactions are balanced.
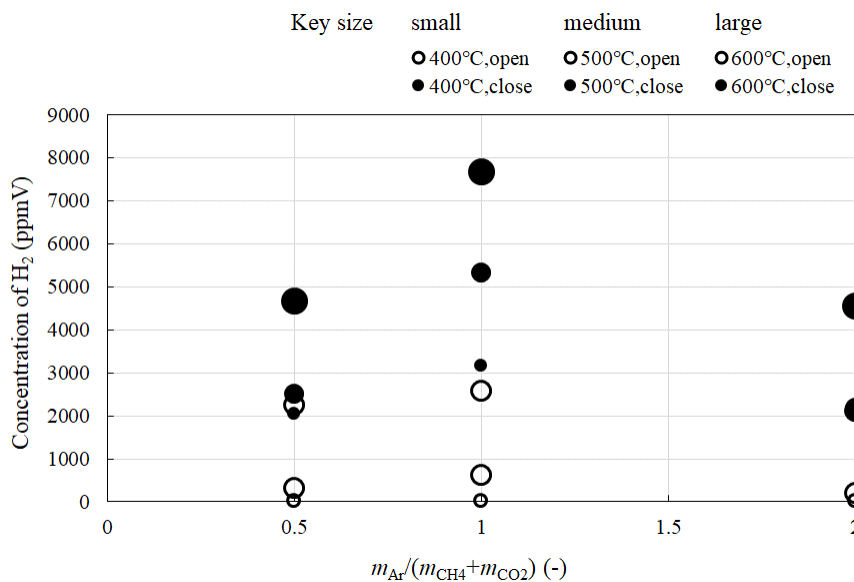

Figure 5 Comparison of the relationship between the concentration of H_2 at the outlet of the reaction chamber and feed ratio of sweep gas with the valve open or close (CH_4 : CO_2 = 1.5 : 1).
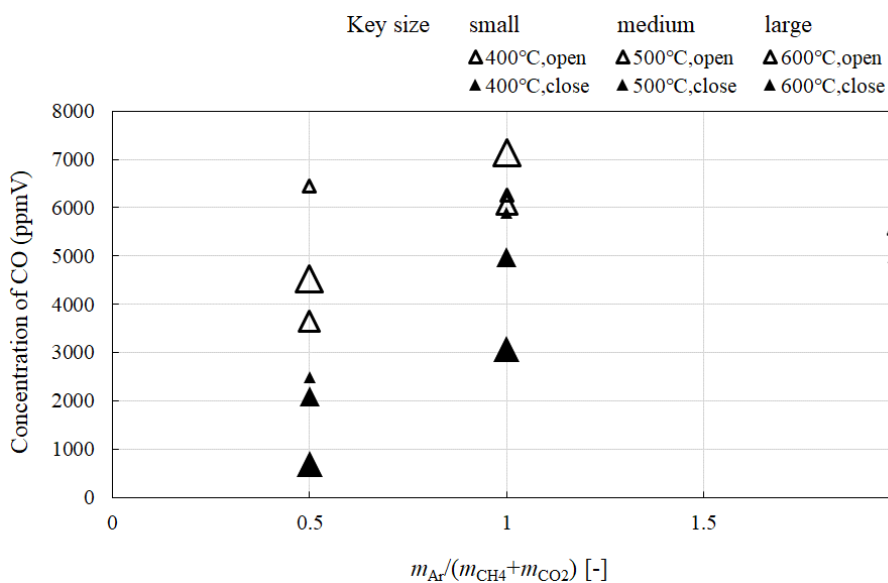

Figure 6 Comparison of the relationship between the concentration of CO at the outlet of the reaction chamber and feed ratio of sweep gas with the valve open or close (CH_4 : CO_2 = 1.5 : 1).
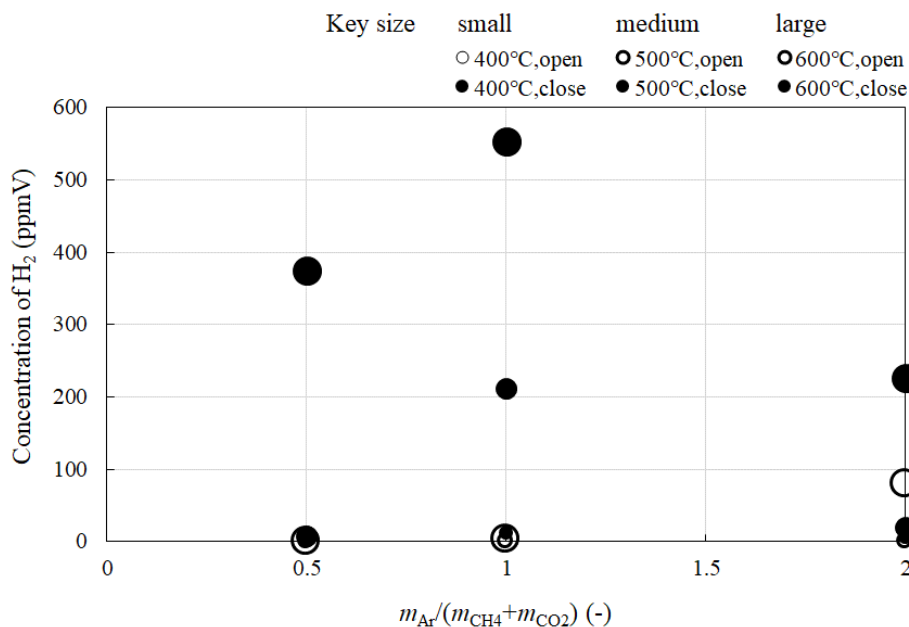
Figure 7 Comparison of the relationship between the concentration of H_2 at the outlet of sweep chamber and feed ratio of sweep gas with the valve open or close ($CH_4 : CO_2$ = 1.5 : 1).

Figure 8 and Figure 9 show the comparison of the relationship between the concentration of H_2 and CO at the outlet of the reaction chamber and $m_{Ar}/(m_{CH4}+m_{CO2})$ when the valve installed at the outlet of the reaction chamber is open or close, respectively. Figure 10 shows the comparison of the relationship between the concentration of H_2 at the outlet of the sweep chamber and $m_{Ar}/(m_{CH4}+m_{CO2})$ when the valve is open or close, respectively. The molar ratio of the supplied $CH_4:CO_2$ is 1:1. The reaction temperature is changed to 400 °C, 500 °C, and 600 °C.

Figure 8 Comparison of the relationship between the concentration of H_2 at the outlet of the reaction chamber and feed ratio of sweep gas with the valve is open or close ($CH_4 : CO_2$ = 1 : 1).
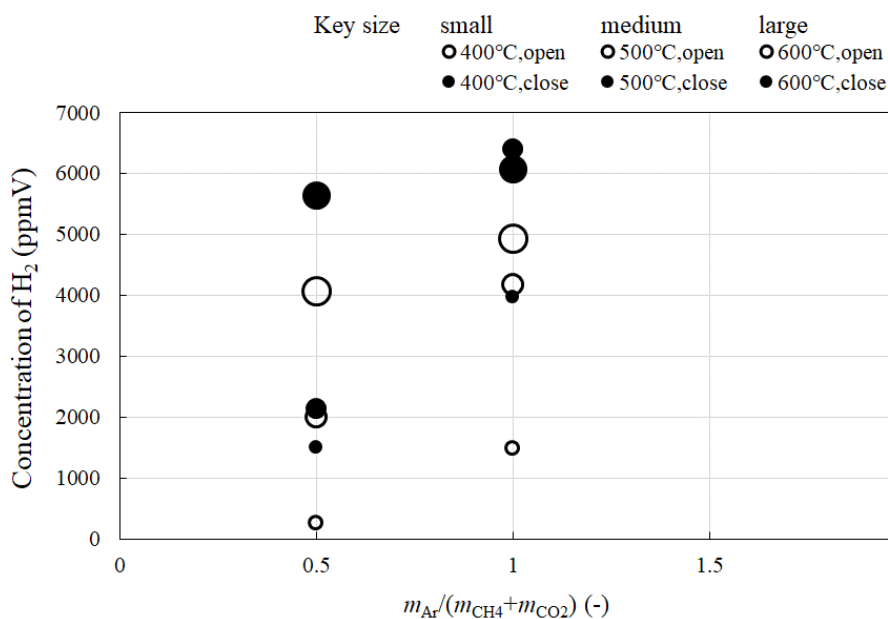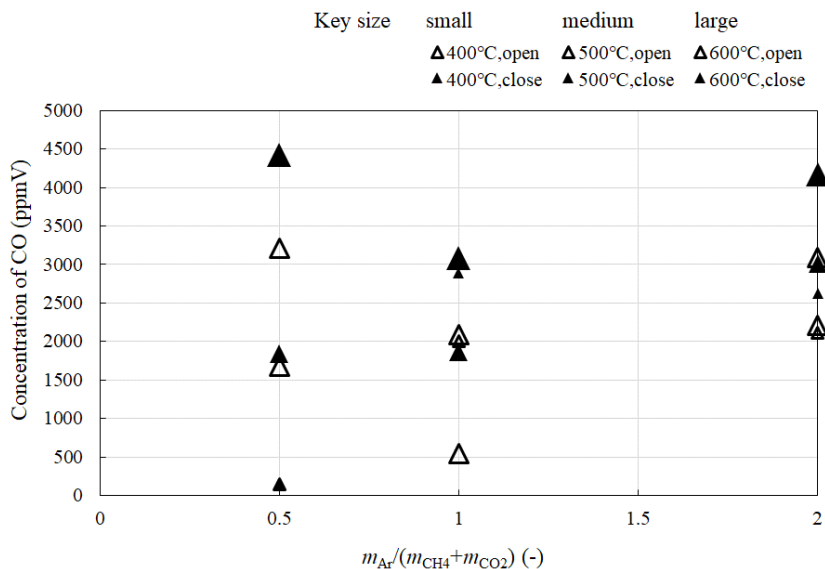
Figure 9 Comparison of the relationship between the concentration of CO at the outlet of the reaction chamber and feed ratio of sweep gas with the valve is open or close ($CH_4 : CO_2 = 1 : 1$).

According to Figures 8 and 10, the concentration of H_2 is higher when the valve is close. Since the pressure difference between the reaction and sweep chambers is higher upon closing the valve, it is thought that the H_2 separation is promoted, resulting in an increase in the concentration of H_2. Also, it is known from Figure 9 that the concentration of CO is higher when the valve is close. Since the molar ratio of the supplied $CH_4:CO_2 = 1:1$ is the same as the theoretical value as shown in Eq. (1), it is believed that the dry reforming progressed well. Besides, it is seen from Figures 8 and 10 that the highest concentration of H_2 is obtained for $m_{Ar}/(m_{CH4}+m_{CO2}) = 1$. It is revealed that the optimum $m_{Ar}/(m_{CH4}+m_{CO2})$ to produce H_2 is 1, and shows the same tendency when the molar ratio of supplied $CH_4:CO_2 = 1.5:1$.
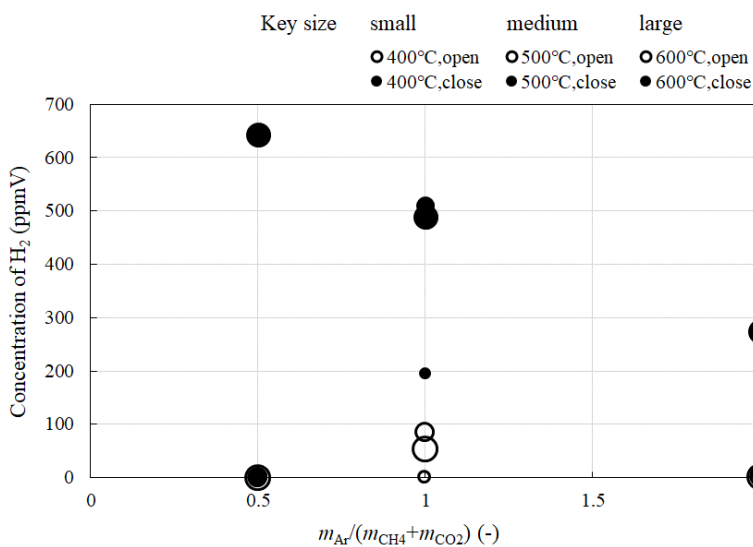

Figure 10 Comparison of the relationship between the concentration of H_2 at the outlet of sweep chamber and feed ratio of sweep gas with the valve is open or close ($CH_4 : CO_2 = 1 : 1$).

Figure 11 and Figure 12 compare the relationship between the concentration of H_2 and CO at the outlet of the reaction chamber and $m_{Ar}/(m_{CH4}+m_{CO2})$, when the valve installed at the outlet of the reaction chamber is open or close, respectively. Figure 13 shows the comparison of the relationship between the concentration of H_2 at the outlet of the sweep chamber and $m_{Ar}/(m_{CH4}+m_{CO2})$ when the valve installed at the outlet of the reaction chamber is open or close, respectively. The molar ratio of the supplied $CH_4:CO_2$ is 1:1.5. The reaction temperature is changed to 400 °C, 500 °C or 600 °C.

According to Figures 11 and 13, the concentration of H_2 is higher when the valve is close. Since the pressure difference between the reaction and sweep chambers is higher when the valve is close, it is thought that H_2 separation is promoted, increasing the concentration of H_2. Additionally, it is seen from Figures 11 and 13 that the highest concentration of H_2 is obtained for $m_{Ar}/(m_{CH4}+m_{CO2}) = 1$. It is revealed that the optimum $m_{Ar}/(m_{CH4}+m_{CO2})$ to produce H_2 is 1, which is also the case when the molar ratio of the supplied $CH_4:CO_2$ = 1.5:1 and 1:1. It is obvious that $m_{Ar}/(m_{CH4}+m_{CO2}) = 1$ is the optimum ratio irrespective of the molar ratio of the supplied $CH_4 : CO_2$, where the reactions are balanced as described above.

According to Figures 3 to 13, the concentrations of produced H_2 and CO are low. This low conversion is thought to be caused by the use of pure Ni as the catalyst. In this study, pure Ni was used to evaluate the basic characteristics of the proposed membrane reactor as the first step to develop the reactor. According to the literature, noble metals such as Pd, Pt [21], and Ru, as well as the alloy of Ni and the other metals, e.g., Co, Cu, Fe, and Ce [28] showed better catalytic activity for the conversion of CH_4 and CO_2 compared to pure Ni. Therefore, this study used other catalysts, as mentioned above, to promote the CH_4 and CO_2 conversion in the proposed membrane reactor as the next step.

Figure 11 Comparison of the relationship between the concentration of H_2 at the outlet of the reaction chamber and feed ratio of sweep gas with the valve is open or close ($CH_4 : CO_2 = 1 : 1.5$).

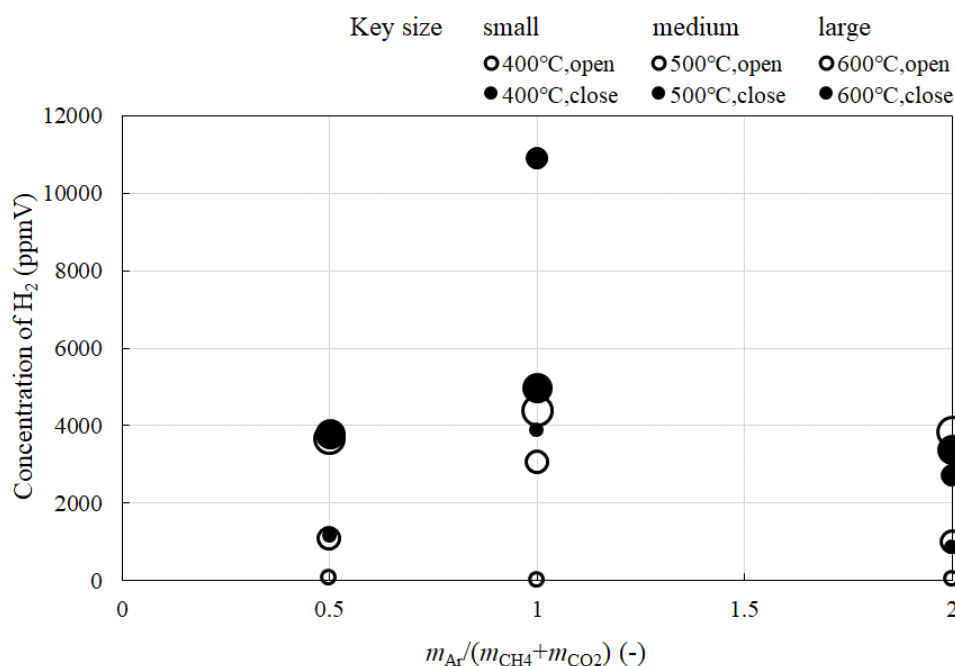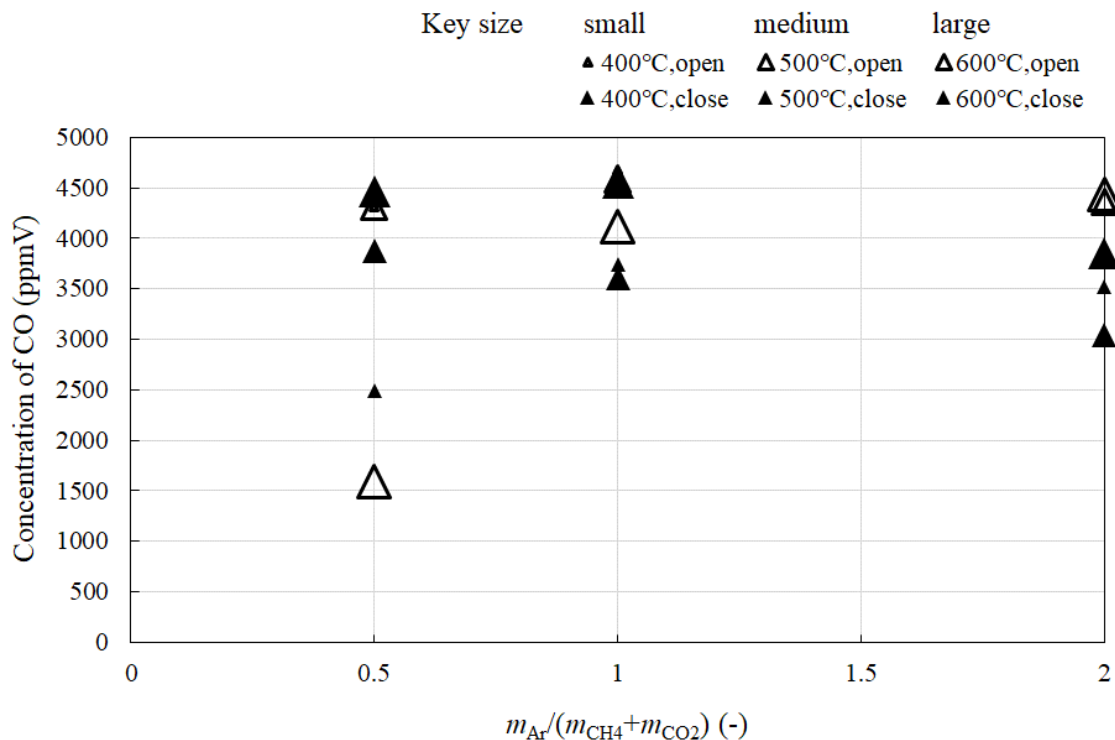**Figure 12** Comparison of the relationship between the concentration of CO at the outlet of the reaction chamber and feed ratio of sweep gas with the valve is open or close ($CH_4 : CO_2 = 1 : 1.5$).
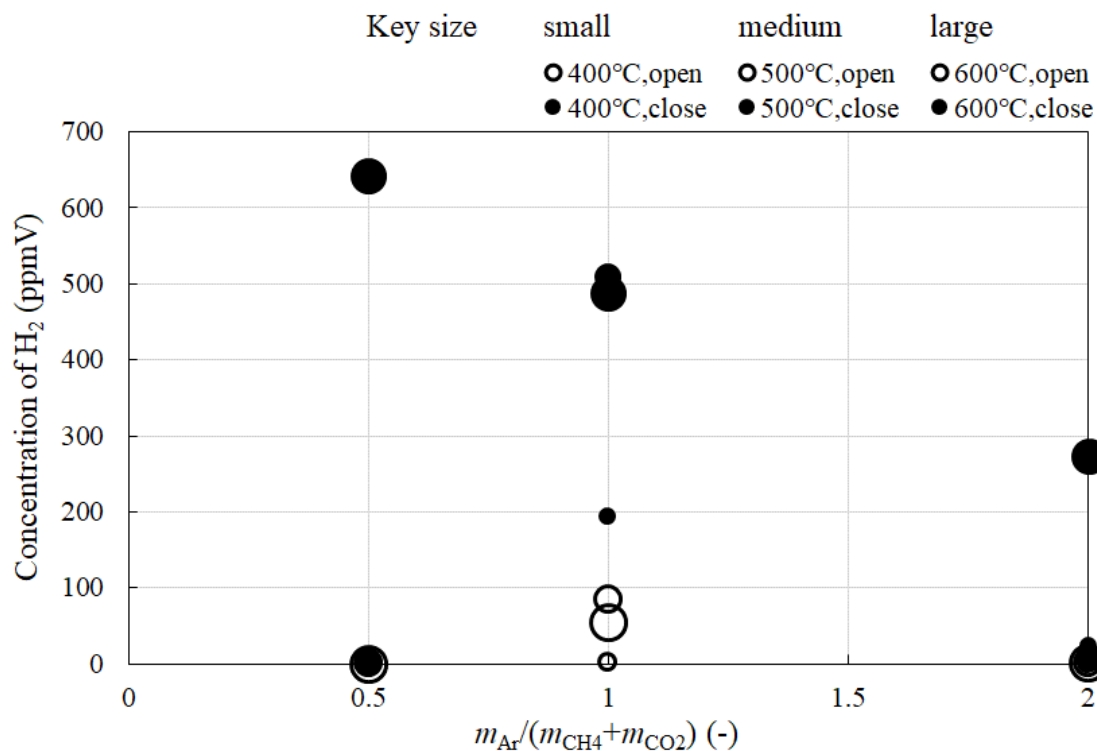

Figure 13 Comparison of the relationship between the concentration of H_2 at the outlet of sweep chamber and feed ratio of sweep gas with the valve is open or close ($CH_4 : CO_2 = 1 : 1.5$).

3.2 Evaluation on Performance of Proposed Reactor

Table 2 and Table 3 list the pressure differences between the reaction and sweep chambers when the molar ratio of $CH_4:CO_2$ = 1.5:1, 1:1, 1:1.5, and the valve at the outlet of the reaction chamber is open or close, respectively. It is seen from the data that the pressure differences are 0 kPa when the valve is open, irrespective of the molar ratio. Since the valve is open, the gases in the reaction chamber might flow out without H_2 separation by the Pd/Cu alloy membrane. This is further confirmed by the concentration of H_2 at the outlet of the sweep chamber, which is almost 0 ppmV, as shown in Figures 7, 10, and 13. When the valve is close, the pressure difference and concentration of H_2 at the outlet of the sweep chamber increase with the rise in the reaction temperature. In other words, closing the valve, i.e., increasing the pressure difference and reaction temperature, promotes the CH_4 dry reforming reaction.

Table 2 Pressure difference between the reaction chamber and the sweep chamber in the case of the molar ratio of $CH_4 : CO_2$ = 1.5 : 1, 1 : 1, 1 : 1.5, with the valve installed at the outlet of the reaction chamber is open (unit: kPa).

$m_{Ar}/$ $(m_{CH4} + m_{CO2})$	$CH_4 : CO_2$								
	1.5 : 1			1 : 1			1 : 1.5		
	400 °C	500 °C	600 °C	400 °C	500 °C	600 °C	400 °C	500 °C	600 °C
0.5	1	0	0	1	0	0	0	0	1
1	0	0	0	0	0	0	0	0	0
2	0	0	0	0	0	0	0	0	0

Table 3 Pressure difference between the reaction chamber and the sweep chamber in the case of the molar ratio of $CH_4 : CO_2$ = 1.5 : 1, 1 : 1, 1 : 1.5, without the valve installed at the outlet of the reaction chamber is open (unit: kPa).

$m_{Ar}/$ $(m_{CH4} + m_{CO2})$	$CH_4 : CO_2$								
	1.5 : 1			1 : 1			1 : 1.5		
	400 °C	500 °C	600 °C	400 °C	500 °C	600 °C	400 °C	500 °C	600 °C
0.5	4	7	8	5	6	7	8	9	10
1	4	7	8	6	6	7	8	9	10
2	4	7	8	5	6	7	8	9	10

Figure 14, Figure 15 and Figure 16 compare the relationship between H_2 or CO selectivity and $m_{Ar}/(m_{CH4}+m_{CO2})$ when the molar ratio of supplied $CH_4:CO_2$ = 1.5:1, 1:1, and 1:1.5, respectively with a closed valve. The reaction temperature is set to 400 °C, 500 °C, and 600 °C, respectively. The figures indicate that H_2 selectivity increases and CO selectivity decreases with an increase in the reaction temperature as the CH_4 dry reforming is an endothermic reaction [9, 35]. According to the previous study [36], the H_2/CO ratio increases with increased reaction temperature because CH_4 dry reforming is an endothermic reaction, which is thermodynamically and kinetically favored at high temperatures.

Besides, these figures show that the CO selectivity is higher than that of H_2 at $m_{Ar}/(m_{CH4}+m_{CO2})$ = 2. If $m_{Ar}/(m_{CH4}+m_{CO2})$ is higher than 2, the biogas dry reforming in the reaction chamber requires longer reaction time.

Figure 14 Comparison of the relationship between H_2 or CO selectivity and feed ratio of sweep gas with the closed valve ($CH_4 : CO_2 = 1.5 : 1$).

Figure 15 Comparison of the relationship between H_2 or CO selectivity and feed ratio of sweep gas with the closed valve ($CH_4 : CO_2 = 1 : 1$).
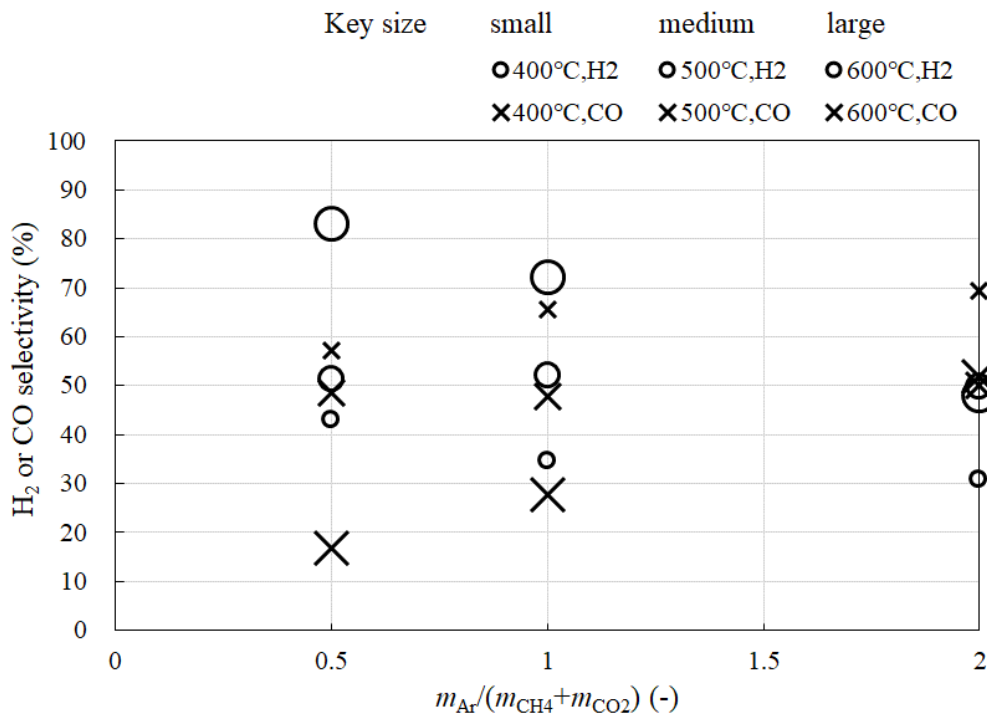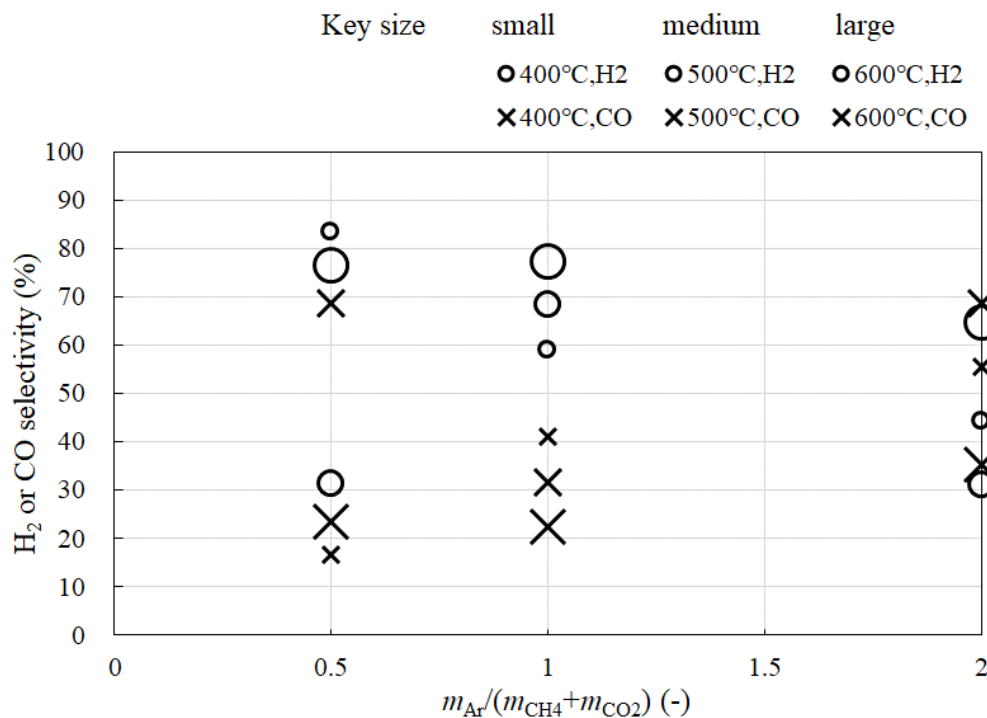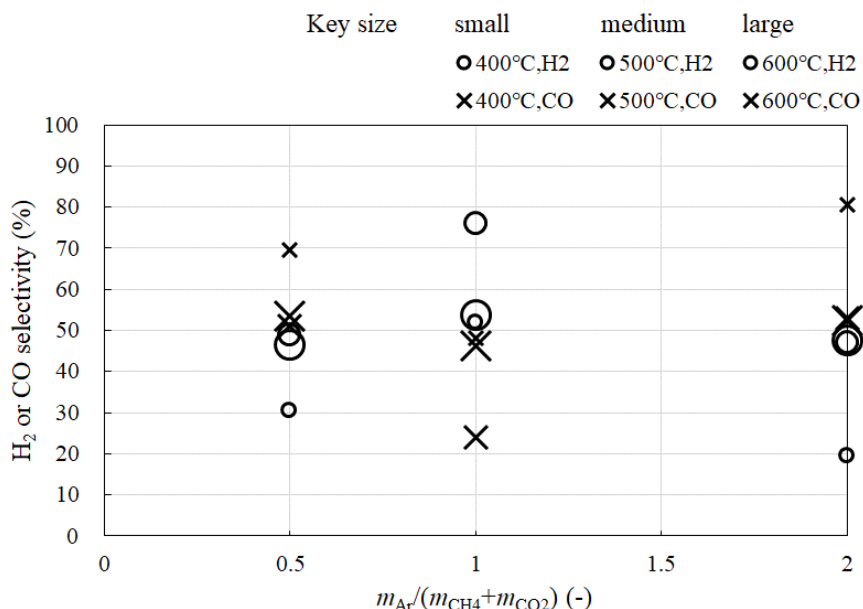
Figure 16 Comparison of the relationship between H_2 or CO selectivity and feed ratio of sweep gas with the closed valve ($CH_4 : CO_2 = 1 : 1.5$).

Table 4 and Table 5 give a comparison of thermal efficiency under different operating conditions when the valve is open and close, respectively. The data show that the thermal efficiency with a closed valve is higher than that when it is open, irrespective of the reaction temperature, $m_{Ar}/(m_{CH4}+m_{CO2})$, and the molar ratio of the supplied CH_4:CO_2. Also, it is revealed that the thermal efficiency at $m_{Ar}/(m_{CH4}+m_{CO2}) = 1$ is higher than any other conditions.

Table 4 Comparison of thermal efficiency among different operation conditions with the open valve (unit: %).

| $m_{Ar}/$ | $CH_4 : CO_2$ | | | | | | | | |
| | 1.5 : 1 | | | 1 : 1 | | | 1 : 1.5 | | |
$(m_{CH4}+m_{CO2})$ (-)	400 °C	500 °C	600 °C	400 °C	500 °C	600 °C	400 °C	500 °C	600 °C
0.5	0	0.3	2.0	0.3	2.2	3.6	0.1	1.2	3.3
1	0	0.6	1.9	1.7	3.8	3.7	0	2.7	3.2
2	0	0.1	1.2	0.1	0.9	1.8	0	0.6	2.1

Table 5 Comparison of thermal efficiency among different operation conditions with the close valve (unit: %).

| $m_{Ar}/$ | $CH_4 : CO_2$ | | | | | | | | |
| | 1.5 : 1 | | | 1 : 1 | | | 1 : 1.5 | | |
$(m_{CH4}+m_{CO2})$ (-)	400 °C	500 °C	600 °C	400 °C	500 °C	600 °C	400 °C	500 °C	600 °C
0.5	2.8	2.7	4.5	2.1	2.3	5.6	1.6	4.2	3.6
1	3.6	4.9	6.1	4.7	6.1	4.8	4.6	10.4	4.0
2	1.7	1.4	2.6	1.7	1.2	3.0	0.7	1.8	1.9

In this study, the thermal efficiencies achieved were not high under different conditions. It is thought that effective H_2 separation was not obtained since the pressure difference between the reaction and sweep chambers was not high enough to extract H_2. As a result, there was no displacement of the thermodynamic equilibrium of the reaction, causing less production of H_2. It is necessary to improve the reaction performance of biogas dry reforming and H_2 separation. Since this study investigated pure Ni catalyst and Ni-based alloy catalyst such as Ni/Ce [10], Ni/La [17], Ni/ZnO-Al$_2$O$_3$ [37], the latter was found to have better performance and can be preferentially used for further studies. Also, the characterization of the H_2 separation membrane, such as composition, thickness, and metal type, is important to improve the efficiency of H_2 separation. Since this study investigated one type of H_2 separation membrane only, i.e., Pd/Cu alloy membrane (Cu of 40 wt%), the composition and thickness of the Pd/Cu alloy membrane will also be investigated in the future.

4. Conclusions

In this paper, the effect of operating conditions such as the feed ratio of the sweep gas, pressure in the reactor, and reaction temperature on the performance of biogas dry reforming was studied. The effects of the molar ratio of the supplied CH$_4$:CO$_2$, as well as $m_{Ar}/(m_{CH4}+m_{CO2})$ on the performance of biogas dry reforming were also investigated. The effects were evaluated by comparing the conditions when the valve was open and close at the outlet of the reaction chamber. The reaction temperature was set to 400 °C, 500 °C, and 600 °C, respectively. The following conclusions are obtained from the study:

1) The final concentration of H_2 in the reaction chamber with closed valve is higher than that with the open valve, irrespective of the molar ratio of supplied CH$_4$:CO$_2$, since H_2 separation is promoted by the increase in the pressure difference between the reaction and sweep chambers.

2) It is confirmed that the optimum $m_{Ar}/(m_{CH4}+m_{CO2})$ to produce H_2 is 1, irrespective of the molar ratio of supplied CH$_4$:CO$_2$.

3) The H_2 selectivity increases and CO selectivity decreases with an increase in the reaction temperature, irrespective of the molar ratio of supplied CH$_4$:CO$_2$.

4) CO selectivity is likely to be higher than H_2 selectivity at $m_{Ar}/(m_{CH4}+m_{CO2})$ = 2 since the separation speed would be higher compared to the reaction speed of biogas dry reforming.

5) The thermal efficiency of the reactor with a closed valve is higher than that with the open valve, irrespective of the reaction temperature, $m_{Ar}/(m_{CH4}+m_{CO2})$, and the molar ratio of supplied CH$_4$:CO$_2$.

6) It is revealed that the thermal efficiency at $m_{Ar}/(m_{CH4}+m_{CO2})$ = 1 is the highest due to maximum H_2 production.

Author Contributions

Akira Nishimura managed this study and wrote the paper; Satoshi Ohata carried out the experiment and collected the data; Kaito Okukura carried out the experiment and collected the data; Eric Hu refined the paper from the view point of native English speaker.

Funding

This work was financially supported by the joint usage/research program of the Institute of Materials and Systems for Sustainability (IMaSS), Nagoya University.

Competing Interests

The authors have declared that no competing interests exist.

References

1. Kalai DY, Stangeland K, Jin Y, Tucho WM, Yu Z. Biogas dry reforming for syngas production on La promoted hydrotalcite-derived Ni catalysts. Int J Hydrogen. 2018; 43: 19438-19450.
2. World Bioenergy Association. Global Bioenergy Statistics. Available from: https://worldbioenergy.org/global-bioenergy-statistics.
3. The Japan Gas Association. Available from: https://www.gas.or.jp/gas-life/biomass/.
4. Jabbour K, Saad A, Inaty L, Davidson A, Massiani P, Hassan NE. Ordered mesoporous Fe-Al$_2$O$_3$ based-catalysts synthesized via a direct "one-pot" method for the dry reforming of a model biogas mixture. Int J Hydrogen Energ. 2019; 44: 14889-14907.
5. Navarro-Puyuelo A, Reyero I, Moral A, Bimbela F, Banares MA, Gandia LM. Effect of oxygen addition, reaction temperature and thermal treatments on syngas production from biogas combined reforming using Rh/alumina catalysts. J Ind Eng Chem. 2019; 80: 21-226.
6. Paksoy AI, Akdag CY, Caglayan BS, Aksoylu AE. Kinetic and mechanistic features of carbon dioxide reforming of methane over Co-Ce/ZrO$_2$ catalysts. Int J Chem Kinet. 2019; 51: 138-145.
7. Hernandez B, Martin M. Optimal production of syngas via super-dry reforming. Analysis for natural gas and biogas under different CO$_2$ taxes. Chem Eng Res Des. 2019; 148: 375-392.
8. Price CAH, Arnold W, Pastor-Perez L, Amini-Horri B, Reina TR. Catalytic upgrading of a biogas model mixture via low temperature DRM using multicomponent catalysts. Top Catal. 2019. DOI: 10.1007/s11244-019-01216-8.
9. Chein R, Yang Z. Experimental study on dry reforming of biogas for syngas production over Ni-based catalysts. ACS Omega. 2019; 4: 20911-20922.
10. Kalai DY, Stangeland K, Tucho WM, Jin Y, Yu Z. Biogas reforming on hydrotalcite-derived Ni-Mg-Al catalysts: The effect of Ni loading and Ce promotion. J CO$_2$ Util. 2019; 33: 189-200.
11. Schiaroli N, Lucarelli C, Luna GS, Fornasari G, Vaccari A. Ni-based catalysts to produce synthesis gas by combined reforming of clean biogas. Appl Catal A Gen. 2019; 582. DOI: 10.1016/j.apcata.2019.05.021.
12. Calgaro, CO, Perez-Lopez OW. Biogas dry reforming for hydrogen production over Ni-M-Al catalysts (M = Mg, Li, Ca, La, Cu, Co, Zn). Int J Hydrogen Energ. 2019; 44: 17750-17766.
13. Rosha P, Mohapatra SK, Mahla SK, Dhir A. Catalytic reforming of synthetic for hydrogen enrichment over Ni supported on ZnO-CeO$_2$ mixed catalyst. Biomass Bioenerg. 2019; 125: 70-78.
14. Rosha P, Mohapatra SK, Mahla SK, Dhir A. Hydrogen enrichment of biogas via dry and autothermal-dry reforming with pure nickel (Ni) nanoparticle. Energy. 2019; 172: 733-739.

15. Sache E, Johnson S, Pastor-Perez L, Horri BA, Reina TR. Biogas upgrading via dry reforming over a Ni-Sn/CeO$_2$-Al$_2$O$_3$ catalyst: Influence of the biogas source. Energies. 2019; 12: 1-14. DOI: 10.3390/en12061007.

16. Rosha P, Mohapatra SK, Mahla SK, Dhir A. Biogas reforming for hydrogen enrichment by ceria decorated over nickel catalyst supported on titania and alumina. Int J Hydrogen Energ. 2018; 43: 21246-21255.

17. Kalai DY, Stangeland K, Jin Y, Tucho WM, Yu Z. Biogas dry reforming for syngas production on La promoted hydrotalcite-derived Ni catalysts. Int J Hydrogen Energ. 2018; 43: 19438-19450.

18. Anzelmo B, Wilcox J, Liguori S. Natural gas steam reforming reaction at low temperature and pressure conditions for hydrogen production via Pd/PSS membrane reactor. J Membrane Sci. 2017; 522: 343-350.

19. Yan Y, Cui Y, Zhang L, Li L, Zhang J, Chen Y, Tang Q, Lin C. Experimental investigation of methane auto-thermal reforming in hydrogen-permeable membrane reactor for pure hydrogen production. Int J Hydrogen Energ. 2016; 41: 13069-13076.

20. Dolan MD, Beath AC, Hla SS, Way JD, Hawa HWAE. An experimental and techno-economic assessment of solar reforming for H$_2$ production. Int J Hydrogen Energ. 2016; 41: 14583-14595.

21. Brunetti A, Fontananova E. CO$_2$ conversion by membrane reactors. J Nanosci Nanotechnol. 2019; 19: 3124-3134.

22. Sumrunronnasak S, Tantayanon S, Kiatgamolchai S, Sukonket T. Improved hydrogen production from dry reforming reaction using a catalytic packed-bed membrane reactor with Ni-based catalyst and dense PdAgCu alloy membrane. Int J Hydrogen Energ. 2016; 41: 2621-2630.

23. Duran P, Sanz-Martinez A, Soler J, Menendez M, Herguido J. Pure hydrogen from biogas: Intensified methane dry reforming in a two-zone fluidized bed reactor using permselective membranes. Chem Eng J. 2019; 370: 772-781.

24. Leimert JM, Karl J, Dillig M. Dry reforming of methane using a nickel membrane reactor. Processes. 2017; 5: 82. DOI: 10.3390/pr5040082.

25. Alexandrov AV, Gavrilova NN, Kislov VR, Skudin VV. Comparison of membrane and conventional reactors under dry methane reforming conditions. Petrol Chem. 2017; 57: 804-812.

26. Lee B, Lim H. Parametric studies for CO$_2$ reforming of methane in a membrane reactor as a new CO$_2$ utilization process. Korean J Chem Eng. 2017; 34: 199-205.

27. Lee B, Lee S, Lim H. Numerical modeling studies for a methane dry reforming in a membrane reactor. J Nat Gas Sci Eng. 2016; 34: 1251-1261.

28. Gao Y, Jiang J, Meng Y, Yan F, Aihemaiti A. A review of recent developments in hydrogen production via biogas dry reforming. Energ Convers Manage. 2018; 171: 133-155.

29. Ugarte P, Duran P, Lasobras J, Soler J, Menendez M, Herguido J. Dry reforming of biogas in fluidized bed: Process intensification. Int J Hydrogen Energ. 2017; 42: 13589-13597.

30. Sunggeun L, Hankwon L. The effect of changing the number of membranes in methane carbon dioxide reforming: A CFD study. J Ind Eng Chem. In press.

31. Wu HC, Rui Z, Lin JYS. Hydrogen production with carbon dioxide capture by dual-phase ceramic-carbonate membrane reactor vis steam reforming of methane. J Membrane Sci. 2020; 598. DOI: 10.1016/j.memsci.2019.117780.

32. Jia H, Xu H, Sheng X, Yang X, Shen W, Goldbach A. High-temperature ethanol steam reforming in PdCu membrane reactor. J Membrane Sci. 2020; 605. DOI: 10.1016/j.memsci.2020.118083.

33. Fontana AD, Faroldi B, Cornaglia LM, Tarditi AM. Development of catalytic membranes over PdAu selective films for hydrogen production through the dry reforming of methane. Mol Catal. 2020; 481. DOI: 10.1016/j.mcat.2018.07.018.

34. Li H, Goldbach A, Li W, Xu H. PdC formation in ultra-thin Pd membrane during separation of H_2/CO mixtures. Int J Hydrogen Energ. 2016; 41: 10193-10201.

35. Karemore AL, Vaidya PD, Sinha R, Chugh P. On the dry and mixed reforming of methane over Ni/Al_2O_3 – Influence of reaction variables on syngas production. Int J Hydrogen Energ. 2016; 41: 22963-22975.

36. Chein RY, Fung WY. Syngas production via dry reforming of methane over CeO_2 modified Ni/Al_2O_3 catalysts. Int J Hydrogen Energ. 2019; 44: 14303-14315.

37. Nataj SMM, Alavi SM, Mazloom G. Catalytic performance of Ni supported on ZnO-Al_2O_3 composites with different Zn content in methane dry reforming. Soc Chem Ind. 2018; 94: 1305-1314.

Enjoy *JEPT* by:

1. Submitting a manuscript
2. Joining in volunteer reviewer bank
3. Joining Editorial Board
4. Guest editing a special issue

For more details, please visit:
http://www.lidsen.com/journal/jept